Synthesis and Monoamine Oxidase Inhibitory Activity of New Pyridazine-, Pyrimidine- and 1,2,4-Triazine-Containing Tricyclic Derivatives

Andrea Carotti,[§] Marco Catto,[§] Francesco Leonetti,[§] Francesco Campagna,[§] Ramón Soto-Otero,[†] Estefanía Méndez-Álvarez,[†] Ulrike Thull,[‡] Bernard Testa,[‡,#] and Cosimo Altomare*[,§]

Dipartimento Farmaco-chimico, University of Bari, Via E. Orabona 4, I-70125 Bari, Italy; Department of Biochemistry and Molecular Biology, University of Santiago de Compostela, S. Francisco 1, E-15782 Santiago de Compostela, Spain; and Institut de Chimie Thérapeutique, Université de Lausanne, BEP, CH-1015 Lausanne, Switzerland

Received June 21, 2007

A number of condensed azines, mostly belonging to the families of indeno-fused pyridazines (**1**), pyrimidines (**2**, **3**), and 1,2,4-triazines (**4**, **5**), were synthesized and evaluated in vitro as monoamine oxidase (MAO) A and B inhibitors. Most of them showed higher inhibition potency toward MAO-B, the most effective one being 3-(3-nitrophenyl)-9*H*-indeno[1,2-*e*] [1,2,4]triazin-9-one (**4c**), which displayed an IC_{50} value of 80 nM and proved to be 10-fold more potent than its [2,1-*e*] fusion isomer **5**. Replacing the 3-phenyl group of the known indeno[1,2-*c*]pyridazin-5-one MAO-B inhibitors with a flexible phenoxymethyl group enhanced the inhibitory potency. The inhibition data highlighted the importance of the aza-heterocyclic scaffold in affecting the MAO isoform selectivity. The 3-phenyl derivatives with type **1**, **4**, and **5** scaffolds were inhibitors of MAO-B with little or no MAO-A effect, whereas 2- or 3-phenyl derivatives of type **2** and **3** pyrimidine-containing fusion isomers inhibited both isoenzymes with a structure-dependent preference toward MAO-A.

Introduction

Monoamine oxidase (MAO) plays a key role in the regulation of various monoamine neurotransmitters such as serotonin (5-HT), norepinephrine (NE), and dopamine (DA).[1] In mammals MAO exists in two isoforms, MAO-A and MAO-B, which are encoded by two different genes.[2−4] Both enzymes are tightly bound to the mitochondrial outer membrane, but albeit sharing about 70% amino acid identity,[5,6] they differ with respect to substrate specificity, sensitivity to inhibitors,[7] and tissue distribution.[8] MAO-A preferentially metabolizes 5-HT, NE, and DA and is selectively inhibited by low concentrations of the acetylenic inhibitor clorgyline, whereas MAO-B has higher affinity toward β-phenylethylamine (PEA) and benzylamine and is selectively and irreversibly inhibited by selegiline (L-deprenyl).

The discovery of reversible and selective inhibitors has renewed the interest toward MAO enzymes as drug targets.[9] Selective and reversible MAO-A inhibitors (MAO-A Is) are used in the treatment of depression and anxiety disorders,[10] whereas MAO-B inhibitors (MAO-B Is) are used as adjuncts in the treatment of Parkinson's disease (PD).[11] MAO-B predominates over MAO-A in the human brain, where MAO-B Is have proven to be beneficial in prolonging the anti-Parkinsonian action of L-DOPA. MAO-B Is, which decrease the rate of MAO-B-catalyzed oxidative deamination and, consequently, the production of reactive oxygen species (ROS), might contribute to the treatment of other neurodegenerative diseases, such as Alzheimer's disease (AD[a]).[12,13] The selective and reversible MAO-A inhibitor moclobemide, and brofaromine as well, and the selective MAO-B inhibitor selegiline are free from the hypertensive crises and cardiac arrhythmias due to the dietary intake of tyramine (the so-called cheese effect), which affected older MAO Is (nonselective, irreversible), such as phenelzine and tranylcypromine (Figure 1).[14]

Our understanding of the MAO structure, regulation, and function has progressed significantly on the basis of cloning and site-directed mutagenesis studies,[15,16] but recently the availability of X-ray crystal structures of purified recombinant human MAO-A[17] and MAO-B,[18−20] in complex with irreversible and reversible inhibitors, has provided a structural basis to MAOs' selective enzyme−ligand recognition and useful information for inhibitor design.[21,22] Due to the relevance to the design and development of MAO-B Is, some of us have recently investigated the impact on inhibitor screening of species-dependent differences between human and rat MAO-B, which have 88.6% sequence identity and differ by only one residue in the binding site (I316 in hMAO-B instead of V316 in rMAO-B).[23]

In the past decade we have reported a diverse series of reversible MAO Is,[24−32] some of which allowed the 5*H*-indeno-[1,2-*c*]pyridazine nucleus (IPD **1**, Chart 1) to be identified as scaffold for promising MAO-B selective inhibitors. Several chemical modifications of IPD derivatives and 3D quantitative structure−activity relationship (3D QSAR) studies have been performed.[25,27]

The 3-(*p*-CF_3-phenyl)-IPD congener (**A**, Chart 2) has been found to be a highly potent inhibitor of rat brain mitochondrial MAO-B, with an IC_{50} value of 90 nM. The importance of the IPD scaffold for reversible MAO inhibition was further supported by other recent papers, which demonstrated potent inhibition of baboon liver mitochondrial MAO-B by compounds **B**[33] and **C**[34] (Chart 2).

Two condensed pyrimidine derivatives (IPM **2** and **3**, Chart 1), that is, 2-phenyl-9*H*-indeno[2,1-*d*]pyrimidin-9-one (**2b**; Y = CO, R′ = C_6H_5) and 2-phenyl-5*H*-indeno[1,2-*d*]pyrimidin-5-one (**3a**; Y = CO, R′ = C_6H_5, R″ = H), were also assayed, and **2b** in particular proved to inhibit MAO isoenzymes with moderate A-selectivity (IC_{50} ca. 2 μM).[27]

In this work, we synthesized new derivatives of indeno-fused azines (Chart 1), namely, pyrimidine (**2** and **3**) and 1,2,4-triazine

* Author to whom correspondence should be addressed (telephone +39-080-5442781; fax +39-080-5442230; e-mail altomare@farmchim.uniba.it).
§ University of Bari.
† University of Santiago de Compostela.
‡ Université de Lausanne.
# Present address: Service de Pharmacie, Centre Hospitalier Universitaire, CH-1011 Lausanne-CHUV, Switzerland.

[a] Abbreviations. AD, Alzheimer's disease; FAD, flavine adenine dinucleotide; IPD, 5*H*-indeno[1,2-*c*]pyridazine; IPM, 9*H*-indeno[2,1-*d*]pyrimidine or 5*H*-indeno[1,2-*d*]pyrimidine; MAO-A, monoamine oxidase A; MAO-B, monoamine oxidase B; PD, Parkinson's disease; PDB, Protein Data Bank; ROS, reactive oxygen species.

10.1021/jm070728r CCC: $37.00
Published on Web 10/02/2007

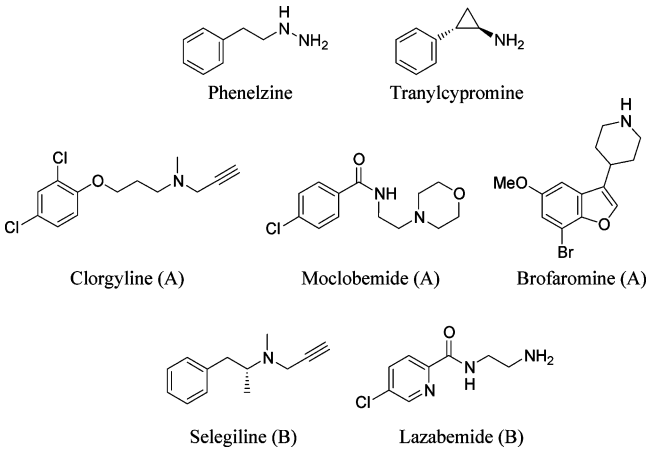

Figure 1. Nonselective and selective MAO-A (A) and MAO-B (B) inhibitors.

Chart 1. Structures and Numbering of the Investigated Indeno-fused Azine Derivatives

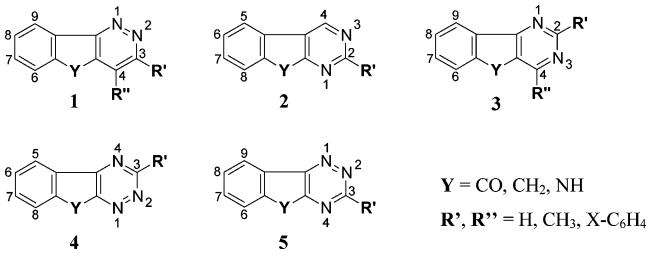

(**4** and **5**), and evaluated them as MAO-A and -B inhibitors. Our investigation was aimed at possibly identifying new scaffolds or lead compounds for the development of reversible and selective MAO Is. A few derivatives of 5*H*-indeno[1,2-*c*]-pyridazin-5-one (**1**, Y = CO) were also examined, which bear at the C-3 position flexible lipophilic side chains, such as phenoxymethyl or benzyloxy groups, instead of a phenyl group.

Results and Discussion

Chemistry. 5*H*-Indeno[1,2-*c*]pyridazin-5-one derivatives bearing *p*-X-substituted (X = H, F, CF_3) phenoxymethyl lateral chains at the C-3 position (**1e**−**g**) were prepared by refluxing the 3-(bromomethyl) derivative **1a′** with the suitable potassium *p*-X-phenoxide in EtOH (Scheme 1).

Benzylation of 3-hydroxy-5*H*-indeno[1,2-*c*]pyridazin-5-one, synthesized according to the method reported by Cignarella et al.,[35] was achieved upon reaction with benzyl bromide in refluxing EtOH in the presence of K_2CO_3 (Scheme 2).

Grignard reaction between 4-benzoylpyridazine[36] and 4-chlorophenylmagnesium chloride gave the alcohol intermediate **1j′**, which was transformed through transposition into [5-(4-cholorophenyl)pyridazin-4-yl](phenyl)methanone (**1j**) by treatment with thionyl chloride.

The preparation of 2-substituted-9*H*-indeno[2,1-*d*]pyrimidin-9-one derivatives, namely, **2a** (R′ = CH_3) and **2d** (R′ = *m*-NO_2-C_6H_4), was accomplished in a three-step procedure according to a method previously reported for the synthesis of compound **2b** (R′ = C_6H_5).[27] A reaction pathway similar to that applied for the synthesis of 4-phenyl-5*H*-indeno[1,2-*d*]pyrimidin-5-one (**3e**) is shown in Scheme 4. 2-[(Dimethylamino)methylen]indan-1-one, prepared by reacting indan-1-one with *N*,*N*-dimethylformamide dimethyl acetal, was treated with an excess of formamidine, in refluxing EtOH in the presence of MeONa, affording 5*H*-indeno[1,2-*d*]pyrimidine **3c**. The reaction of **3c** with phenyllithium yielded the 4-phenyl derivative **3d**, which subsequently underwent oxidation with CrO_3 to compound **3e**.

The 9*H*-indeno[1,2-*e*][1,2,4]triazin-9-one derivatives **4a**−**c** were synthesized according to the reactions shown in Scheme 5. Following a described method,[37] the *m*-nitrophenyl congener **4c** was obtained in almost quantitative yield through a one-pot procedure, reacting ninhydrin and 3-nitrobenzenecarboximidohydrazide in refluxing EtOH for 30 min. Because the NMR spectra of **4c** did not allow the ring fusion isomerism (i.e., [1,2-*e*] versus [2,1-*e*]) to be unambiguously assessed, we isolated the hydrazone intermediate, carrying out the reaction in AcOEt as solvent at 0 °C. As soon as the reagents disappeared (ca. 30 min, TLC check) a dark yellow solid was obtained. Its ^{13}C NMR spectrum (DMSO-d_6 as solvent) showed only one peak at 199.4 ppm, in the ketone carbon downfield characteristic region, which can be assigned to the two equiv C═O groups [note that C(2)═N absorbs at 136.5 ppm], and a peak at 142.4 ppm due to the equivalent substituted aromatic carbons of the indanone moiety. These findings proved the formation of the 1,3-dioxo regioisomer, namely, *N′*-(1,3-dioxo-1,3-dihydro-2*H*-inden-2-ylidene)-3-nitrobenzenecarboximidohydrazide, shown in Scheme 5 as the largely prevailing tautomer form, which is quite stable in solution at −20 °C but underwent rapid cyclization to **4c** in EtOH even at 4 °C.

Reduction of the nitro group in **4c** with $SnCl_2$ in EtOH gave the amino derivative **4b**, which afforded the unsubstituted congener **4a** through acid decomposition of the corresponding diazonium salt.

The fusion isomer 3-(3-nitrophenyl)-5*H*-indeno[2,1-*e*][1,2,4]-triazin-5-one (**5**) was synthesized in good yield according to the synthetic pathway shown in Scheme 6. The reaction between the carboximidohydrazide and indan-1,3-dione afforded the hydrazone intermediate **5′**, which rapidly underwent CH_2 oxidation to CO with CrO_3 and cyclization to compound **5**. The fusion isomers **4c** and **5** showed very similar ^1H NMR spectra in DMSO-d_6 solvent, with chemical shifts slightly higher for the isomer **5**, in line with expectations (e.g., δ 9.25 and 9.45 for **4c** and **5**, respectively).

2-Phenyl-2*H*-indeno[1,2-*c*]pyridazine-3,5-dione (**1k**) was prepared according to procedures reported by some of us (Chart 3).[38] The indole-containing compound **6**, 11*H*-indolo[3,2-*c*]-cinnoline, was kindly made available to us by Prof. G. Cirincione (University of Palermo, Italy), whereas 5,11-dihydro-6*H*-benzo[*a*]carbazole **7** described earlier by Ghigi[39] was synthesized according to a classical Fisher indole synthesis as modified by Pappa et al.[40]

MAO Inhibition and Qualitative SAR. The IC_{50} values of the newly synthesized compounds were obtained by measuring their MAO inhibitory activities in rat brain mitochondria, with a continuous spectrophotometric assay[24] that monitors the rate of oxidation of kynuramine into 4-hydroxyquinoline. To determine the effects of the test compounds on single isoforms, clorgyline and selegiline (both at 250 nM) were used to irreversibly inhibit MAO-A and -B, respectively. The MAO inhibitory activities, expressed as IC_{50} values or percent inhibition at maximum solubility in the assay mixtures, are summarized in Table 1 together with data previously obtained in the same experimental conditions, reported herein to highlight SARs.

Most of the newly synthesized compounds proved to inhibit preferentially MAO-B, some of their potencies being in the low micromolar (**1e** and **1f**) to sub-micromolar (**4c** and **5**) range. As for the heterocyclic scaffold, the experimental data show that the 3-phenyl indeno-triazine (**4a**) is a more potent MAO-B

Chart 2. 5*H*-Indeno[1,2-*c*]pyridazine Derivatives Found as Potent MAO-B Inhibitors

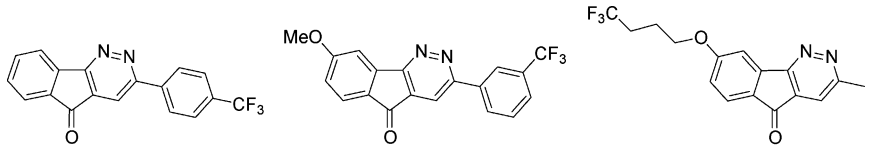

A **B** **C**

Scheme 1[a]

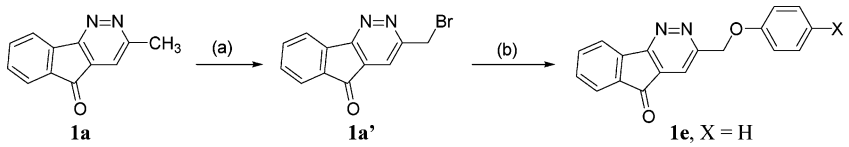

1a **1a'**

1e, X = H

1f, X = F

1g, X = CF_3

[a] Reagents and conditions: (a) NBS, CCl_4, Δ, 2 h; (b) 4-X-$C_6H_4O^-K^+$, EtOH, Δ, 30 min.

Scheme 2[a]

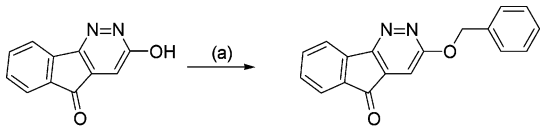

1h

[a] Reagents and conditions: (a) $PhCH_2Br$, K_2CO_3, EtOH, Δ, 30 min.

Scheme 3[a]

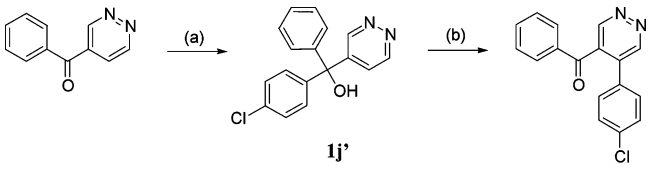

1j' **1j**

[a] Reagents and conditions: (a) 4-ClC_6H_4MgBr, $CeCl_3$, THF, 0 °C, 1.5 h; (b) $SOCl_2$, 50 °C, 15 min.

Scheme 4[a]

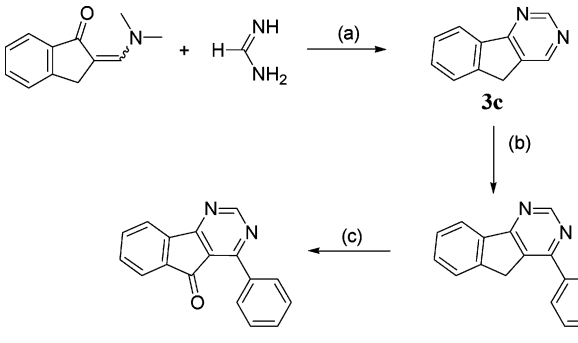

3c **3d** **3e**

[a] Reagents and conditions: (a) MeONa, EtOH, Δ, 48 h; (b) C_6H_5Li, THF, rt, 7 h; (c) CrO_3, HOAc, Δ, 20 min.

inhibitor than the corresponding IPD (**1b**) and IPM (**2b**, **3a**) analogues. In contrast, the IPM analogues (**2b**, **3a**) are slightly selective MAO-A inhibitors. Although none of these compounds were more potent than our previously reported most potent inhibitors, the data in Table 1 significantly add to our knowledge on structure−activity−selectivity relations of condensed azines.

The IPD derivatives **1e**−**h** inhibited selectively MAO-B, with moderate-to-low potencies. The phenoxymethyl side chain in **1e** (but not the benzyloxy group in **1h**) at the C-3 position enhanced MAO-B inhibitory potency by nearly 1 order of magnitude over **1b** bearing the phenyl group. The *p*-F substituent (**1f**) slightly enhanced the inhibitory activity of **1e**, whereas the *p*-CF_3 group (**1g**) proved to be detrimental, most likely because of steric limitations in the substrate binding cavity of MAO-B, as highlighted also by previous studies on rigid selective inhibitors[41] and 3D QSAR models of MAO-mediated bioactivation of analogues of the dopaminergic neurotoxin *N*-methyl-4-phenyl-1,2,3,6-tetrahydropyridine (MPTP).[42]

The open pyridazine derivative **1j**, which was as active as the rigid deschloro analogue **1i**, displayed low MAO-B inhibition and a selectivity reversal toward the A isoform. Even though the MAO-A inhibition potencies of **1i** and **1j** are not worthy of note, the data suggest that a 4-phenyl substituent, irrespective of the rigidity and planarity of the heterocyclic scaffold, favors a preferential affinity to MAO-A.

A significant decrease of MAO-B inhibitory potency and selectivity was also observed with the 2-phenyl-2*H*-indeno[1,2-*c*]pyridazine derivative **1k**, which shows unique structural features and the lowest lipophilicity[43] in the series. Indeed, our previous QSAR studies showed that lipophilicity plays a major role in modulating MAO-B inhibition by structurally diverse heterocyclic compounds.[25,27,28,31]

3-Phenyl-9*H*-indeno[1,2-*e*][1,2,4]triazin-9-one (**4a**) proved to be a more promising scaffold for MAO-B inhibition than the corresponding IPD (**1b**) and IPM (**2b**, **3a**) analogues, and the *m*-NO_2-phenyl congener **4c** was indeed the most potent MAO-B inhibitor found in this study (IC_{50} = 80 nM). Interestingly, its inhibitory potency was 1 order of magnitude higher than that of its [2,1-*e*] fusion isomer **5** (IC_{50} = 912 nM), whereas the favorable effect of the electron-withdrawing nitro group at the meta position of the 3-phenyl group was clearly demonstrated by a >80-fold increase in inhibitory potency of **4c** compared with the unsubstituted (**4a**) and amino (**4b**) congeners.

Molecular Modeling. The best inhibitor **4c** was docked into the binding site of a MAO-B structure. Among the available X-ray crystallographic 3D structures of MAO-B, the complex of human MAO-B with the non-covalent ligand 1,4-diphenyl-2-butene (pdb code 1oj9) was retrieved from the Brookhaven Protein Data Bank and used in the calculations.[20] Analysis of crystal structures of hMAO-B in complex with several inhibitors[19] revealed that the binding site consists of two distinct cavities of different volumes: a larger "substrate cavity" (>400 Å^3), which is located in the vicinity of the flavine adenine dinucleotide cofactor (FAD), and a smaller cavity (nearly 300

Scheme 5[a]

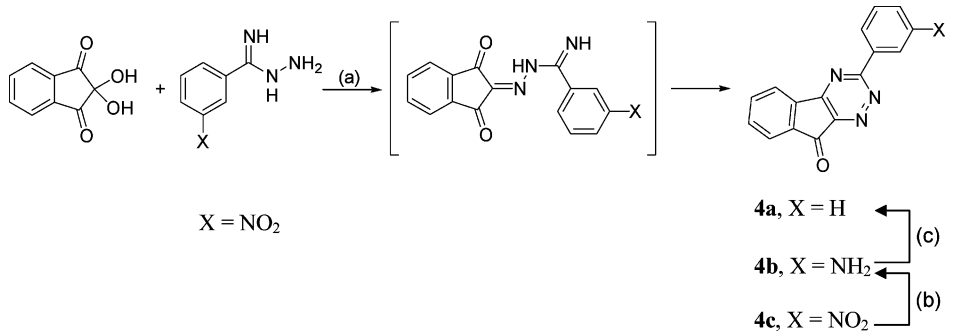

[a] Reagents and conditions: (a) EtOH, Δ, 30 min; (b) $SnCl_2$, EtOH, Δ, 1.5 h; (c) (i) *tert*-butyl nitrite, DMF, 70 °C, 15 min; (ii) H^+, 0 °C.

Scheme 6[a]

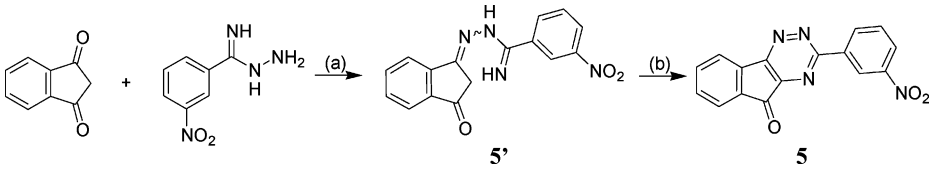

[a] Reagents and conditions: (a) EtOH, Δ, 2 h; (b) CrO_3, HOAc, Δ, 2 h.

Chart 3. Further Condensed Aza-heterocyclic Derivatives Evaluated as MAO Inhibitors

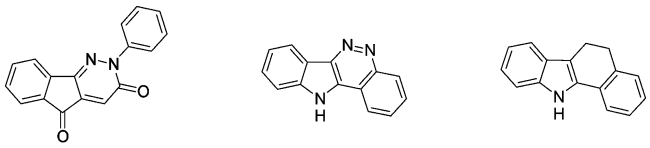

1k **6** **7**

Table 1. In Vitro MAO Inhibition Data (General Structures in Chart 1)

				IC$_{50}$ (μM) or % inhibition[a] (at μM)	
compd	R′	R″	Y	MAO-A	MAO-B
1a	CH_3	H	CO	>100[b]	74.4[b]
1b	C_6H_5	H	CO	0% (20)[b]	21.0[b]
1c	C_6H_5	H	CH_2	>100[b]	23.4[b]
1d	C_6H_5	H	NH	0% (5)[c]	0% (5)[c]
1e	$CH_2OC_6H_5$	H	CO	0% (10)	2.51 ± 0.09
1f	$CH_2O(4'\text{-}F)C_6H_4$	H	CO	12% (10)	1.90 ± 0.71
1g	$CH_2O(4'\text{-}CF_3)C_6H_4$	H	CO	0% (10)	48% (10)
1h	$OCH_2C_6H_5$	H	CO	>100	55.0 ± 3.2
1i	H	C_6H_5	CO	34.3[b]	93.7[b]
1j[d]	H	4′-Cl-C_6H_4	CO	30.8 ± 3.8	>100
1k	*e*		CO	46% (50)	38.0 ± 5.0
2a	CH_3		CO	47.1 ± 7.6	9.40 ± 1.12
2b	C_6H_5		CO	2.37[c]	11.6[c]
2c	C_6H_5		CH_2	16.7 ± 2.5	13.0 ± 0.9
2d	3′-NO_2-C_6H_4		CO	5% (1)	12% (1)
3a	C_6H_5	H	CO	8.39[c]	28% (10)[c]
3b	C_6H_5	H	CH_2	18.0 ± 2.1	37% (20)
3e	H	C_6H_5	CO	21.6 ± 1.4	34.0 ± 4.8
4a	C_6H_5		CO	21% (10)	6.31 ± 0.84
4b	3′-NH_2-C_6H_4		CO	12% (10)	17% (10)
4c	3′-NO_2-C_6H_4		CO	23% (10)	0.080 ± 0.0045
5	3′-NO_2-C_6H_4		CO	3% (10)	0.912 ± 0.011
6	*e*		NH	29.7 ± 5.7	29% (50)
7	*e*		NH	12.0 ± 2.8	38% (25)

[a] The IC$_{50}$ values (100 μM maximum concentration tested) or average percent inhibition at maximum solubility of the inhibitor in the assay conditions (in parentheses) were determined in rat brain mitochondrial suspension. Data are means ± SEM of three experiments, each performed in duplicate. [b] Data (relative SEM < 10%) taken from ref 25. [c] Taken from ref 27. [d] Structure in Scheme 3. [e] Structures in Chart 3.

Å^3), the so-called "entrance cavity", which connects the substrate cavity to the protein surface. These two cavities are separated by residues Y326, I199, L171, and F168, with I199 and Y326 behaving as gate-keepers protecting the catalytic region from the outside. Three conserved water molecules have been identified, which are buried in the vicinity of FAD and proved to be important for docking simulation and virtual screening of MAO-B selective ligands.[23] Two water molecules are involved in a number of H-bonds (wat1 and wat2), whereas a third one (wat3) is kept by the π-system between Y398 and Y435, as well as the central heterocyclic conjugated ring of FAD.

Docking calculations of **4c** into the binding site of hMAO-B were carried out using the QXP software,[44] and the docking pose corresponding to the highest scored solution is shown in Figure 2. In the lowest energy binding pose, the 3-nitrophenyl group is located in the substrate cavity near the FAD cofactor, with a number H-bonds taking place between the NO_2 group and the phenolic OH groups of Y398 and Y435 as well as the carboxamide NH of Q206. The indeno[1,2-*e*][1,2,4]triazin-9-one nucleus is accommodated at the boundary between the entrance and the substrate cavities, where N(1) and N(2) of the triazine ring can form H-bonds with Y326, whereas the indeno ring can interact with the hydrophobic side chains of I199, F103, F168, and W119. Within a range of <1 kcal·mol^{-1} from the best-scored solution, **4c** adopts, following just minor positioning adjustments, similar docking orientations (23 first-ranked solutions of all 25 solutions generated), with the 3-NO_2-phenyl group embedded into the substrate cavity and indeno-triazine nucleus pointing toward the entrance cavity.

On the basis of QXP calculations, the fusion isomer **5** (results not shown) should also interact with the MAO-B binding site in a similar docking pose, but with the planar triazine-containing tricycle rotated by ca. 180° compared to the isomeric nucleus in **4c**.

For the potent indeno[1,2,4]triazine-containing MAO-B inhibitors our docking calculations generated binding modes similar to those previously obtained with 3-X-phenyl IPD inhibitors (type **1** compounds),[23] using the same enzyme structure but a different procedure that consisted of docking calculation with the program GOLD (Genetic Optimization for Ligand Docking)[46] and MLP (Molecular Lipophilicity Potential)[47] fitting point filtering.

The highest MAO-A inhibitory potency was displayed by the IPM derivative **2b** (IC$_{50}$ = 2.37 μM),[27] which moderately

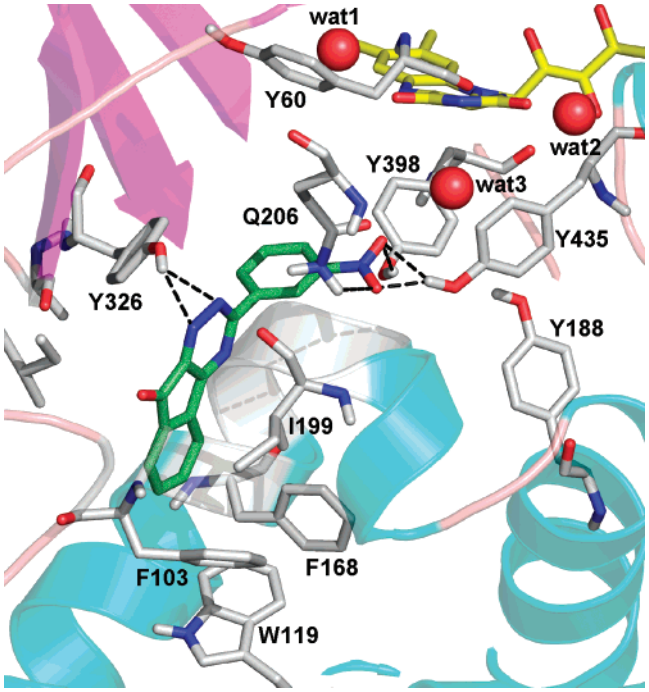

Figure 2. QXP best-scored docking solution of 3-(3-nitrophenyl)-9*H*-indeno[1,2-*e*][1,2,4]triazin-9-one (**4c**) into the binding site of hMAO-B (pdb code: 1oj9). The figure was drawn by PyMOL.[45] The protein is shown in ribbon, and the ligand **4c**, FAD cofactor, and potentially interacting residues in stick (blue, nitrogen; red, oxygen; yellow, carbon atoms in FAD; green, carbon atoms in **4c**). The water molecules retained in the calculation as an integral part of the MAO-B structure are represented as red spheres.

inhibits also the B isoform. Lipophilicity appears to be involved in the modulation of MAO-A inhibitory activity by these congeners. Indeed, the reduction of the carbonyl group of **2b** to methylene (**2c**) significantly diminished MAO-A (but not MAO-B) inhibitory potency (a similar effect was observed also with the fusion isomer **3a**); the replacement of a phenyl (**2b**) with a methyl group (**2a**) resulted even in selecivity reversal, whereas unfortunately introduction of the *meta*-NO_2 substituent on the 2-phenyl group (**2d**) decreased solubility, preventing us from obtaining a finite IC_{50} value. Taking these and previous results into account, 2-phenyl-9*H*-indeno[2,1-*d*]pyrimidin-9-one **2b** emerged as a lead structure for inhibitors of both the isoenzymes.

Finally, the MAO inhibitory potencies of the indole-containing derivatives **6** and **7** were also investigated. Interestingly, 11*H*-indolo[3,2-*c*]cinnoline **6**, which incorporates the pyridazine ring into its structure, and even more interestingly 5,11-dihydro-6*H*-benzo[*a*]carbazole **7**, which (like effective indole-containing inhibitors, e.g., pirlindole, metralindole)[48] does not contain the endocyclic N−N functionality, preferentially inhibit the MAO-A isoform with modest yet significant MAO-A inhibitory potencies (IC_{50} = 29.7 and 12.0 μM for **6** and **7**, respectively). However, these values are higher than those previously determined for 3-phenyl-5*H*-pyridazino[4,3-*b*]indole (**1d**).[27]

Conclusions

The results of this study on the MAO effects of a number of diverse indeno- and indol-fused azines add to our knowledge of structure−activity relationships of azaheterocyclic MAO inhibitors. The preference toward the MAO isoenzymes proved to be dependent on the type of azine-containing tricyclic scaffold. Indeed, the 3-phenyl derivative of 9*H*-indeno[1,2-*e*]-[1,2,4]triazin-9-one (**4a**) is a MAO-B inhibitor more potent than the 5*H*-indeno[1,2-*c*]pyridazin-5-one analogue (**1b**), whereas the indeno-pyrimidinone fusion isomers (**2b** and **3a**) moderately inhibit both MAO isoenzymes with a preference toward MAO-A. Such a preference is favored by the presence of the carbonyl group at the 9-position (**2b**), because its reduction to methylene (**2c**) decreased the MAO-A (but not the MAO-B) inhibitory potency. In addition, as for the MAO-B-selective inhibitors built on the known 5*H*-indeno[1,2-*c*]pyridazin-5-one scaffold, replacing the phenyl group at the C-3 position (**1b**) with a phenoxymethyl chain (**1e**−**g**) significantly enhanced MAO-B inhibitory potency.

A major outcome of this study was the identification of 3-(3-nitrophenyl)-9*H*-indeno[1,2-*e*][1,2,4]triazin-9-one **4c** as a new promising MAO-B selective inhibitor (IC_{50} = 80 nM), which proved to be 10-fold more potent than its fusion isomer **5**. Docking simulation of **4c** into the active site of a hMAO-B suggested a binding mode which, similarly to that previously found for 3-X-phenyl-5*H*-indeno[1,2-*c*]pyridazin-5-one analogues,[23] involves key interactions in the catalytic pocket for MAO-B effective inhibition.

Experimental Section

Chemistry. Melting points were determined by using the capillary method on a Stuart Scientific SMP3 electrothermal apparatus and are uncorrected. Elemental analyses (C, H, N) were performed on a Euroea 3000 analyzer, and the results agreed to within ±0.40% of the theoretical values. IR spectra were recorded using potassium bromide disks on a Perkin-Elmer Spectrum One FT-IR spectrophotometer. Only the most significant IR absorption bands are listed. ^{1}H NMR spectra were recorded at 300 MHz on a Varian Mercury 300 instrument. Chemical shifts are expressed in δ and the coupling constants J in hertz. The following abbreviations are used: s, singlet; d, doublet; t, triplet; dd, double doublet; dt, double triplet; td, triple doublet; tt, triple triplet; ddd, double double doublet; m, multiplet. Signals due to NH protons were located by deuterium exchange with D_2O.

Chromatographic separations were performed on silica gel (15−40 mesh, Merck). Starting materials, unless otherwise stated, were purchased from Sigma-Aldrich. Several compounds were synthesized according to reported procedures with slight modifications, and no effort was made at this stage to optimize the yields. Melting points and spectral data were in full agreement with those reported in literature.

3-(Bromomethyl)-5*H*-indeno[1,2-*c*]pyridazin-5-one (1a′). *N*-Bromosuccinimide (0.250 g, 1.4 mmol) and a catalytic amount of 2,2′-azobis(2-methylpropionitrile) were added to a solution of 3-methyl-5*H*-indeno[1,2-*c*]pyridazin-5-one **1a**[25] (0.196 g, 1 mmol) in 9 mL of CCl_4. The reaction mixture was refluxed for 2 h and then allowed to cool to rt. After the evaporation of the solvent under reduced pressure, the oily residue was purified by column chromatography on silica gel (hexane/ethyl acetate 50:50 v/v, as eluent) giving 0.124 g of **1a′** as a yellow solid (45% yield), which was characterized via GC-MS and NMR and used without further purification.

3-(4-X-Phenoxymethyl)-5*H*-indeno[1,2-*c*]pyridazin-5-one (1e−g). General Procedure. The suitable potassium phenoxide (1.5 mmol) was added to a solution of **1a′** (0.274 g, 1 mmol) in 20 mL of dry EtOH, and the reaction mixture was refluxed for 30 min. The solution was evaporated to dryness, and the crude residue was suspended in water and extracted three times with $CHCl_3$. The organic extracts, collected and washed with water, were dried over Na_2SO_4 and evaporated to dryness. The solid was purified by flash chromatography on silica gel ($CHCl_3$/AcOEt/petroleum ether 80:10:10 v/v/v, as eluent) and crystallized.

1e (X = H): yellow solid, 46% yield; mp 189−190 °C, from $CHCl_3$/AcOEt; ^{1}H NMR ($CDCl_3$) δ 5.46 (s, 2H), 6.96−7.02 (m, 3H), 7.26−7.33 (m, 2H), 7.55 (td, 1H, J = 7.4, 0.9), 7.73 (td, 1H, J = 7.6, 1.1), 7.82−7.85 (m, 1H), 7.86 (s, 1H), 8.16 (d, 1H, J = 7.6); IR (cm^{-1}) 1720, 1420, 1245. Anal. ($C_{18}H_{12}N_2O_2$) C, H, N.

1f (X = F): yellow solid, 28% yield; mp 168 °C (dec) from EtOH; ^{1}H NMR ($CDCl_3$) δ 5.48 (s, 2H), 6.95−7.05 (m, 4H), 7.63 (td, 1H, J = 7.4, 0.8), 7.79 (td, 1H, J = 7.5, 1.1), 7.89 (d, 1H, J = 7.4), 7.89 (s, 1H), 8.31 (d, 1H, J = 7.5); IR (cm^{-1}) 1722, 1506, 1214. Anal. ($C_{18}H_{11}FN_2O_2$) C, H, N.

1g (X = CF_3): yellow solid, 22% yield; mp 181 °C (dec) from EtOH; ^{1}H NMR ($CDCl_3$) δ 5.54 (s, 2H), 7.11 (d, 2H, J = 9.0), 7.59 (d, 2H, J = 9.0), 7.60 (td, 1H, J = 7.4, 0.8), 7.78 (td, 1H, J = 7.4, 1.1), 7.87 (d, 1H, J = 7.4), 7.89 (s, 1H), 8.24 (d, 1H, J = 7.4); IR (cm^{-1}) 1732, 1331, 1110. Anal. ($C_{19}H_{11}F_3N_2O_2$) C, H, N.

3-(Benzyloxy)-5*H*-indeno[1,2-*c*]pyridazin-5-one (1h). To a stirred solution of 3-hydroxy-5*H*-indeno[1,2-*c*]pyridazin-5-one (0.396 g, 2 mmol), prepared according a reported procedure,[35] in 20 mL of EtOH, were added K_2CO_3 (0.276 g, 2 mmol) and excess of benzyl bromide (1.03 g, 6 mmol). The reaction mixture was refluxed for 30 min and, after cooling to rt, filtered through a Celite pad. The obtained product **1h** crystallized from EtOH in 40% yield: mp 169−70 °C; ^{1}H NMR ($CDCl_3$) δ 5.34 (s, 2H), 7.18 (s, 1H), 7.25−7.38 (m, 3H), 7.45−7.48 (m, 2H), 7.51 (td, 1H, J = 7.5, 1.0), 7.71 (td, 1H, J = 7.5, 1.0), 7.82−7.92 (m, 2H); IR (cm^{-1}) 1720, 1610, 1420, 1220. Anal. ($C_{18}H_{12}N_2O_2$) C, H, N.

[5-(4-Chlorophenyl)pyridazin-4-yl](phenyl)methanone (1j). 4-Benzoylpyridazine afforded (4-chlorophenyl)(phenyl)pyridazin-4-ylmethanol **1j′**, via a classical Grignard reaction as modified by Imamoto et al.[49] To a stirred suspension of cerium chloride (1.48 g, 6 mmol) in 13 mL of anhydrous THF was added 6.0 mL of a 1.0 M solution of 4-chlorophenylmagnesium bromide in Et_2O. The mixture was stirred at 0 °C for 1.5 h, and then a solution of 0.37 g of 4-benzoylpyridazine (2.0 mmol) in 20 mL of anhydrous THF was added. After 1 h of stirring at 0 °C, 30 mL of 1 M NH_4Cl was added and the reaction mixture extracted with $CHCl_3$. From the dried organic layer an oily residue was obtained and purified by silica gel chromatography using AcOEt/hexane/isopropyl alcohol (20:75:5 v/v/v) as eluent. The crude product **1j′** (47% yield) was used in the following reaction without further purification.

Compound **1j′** (101 mg, 0.34 mmol) in 1 mL of thionyl chloride was heated in a water bath at 50 °C for 15 min. The reaction mixture was evaporated to dryness and the oily residue purified by silica gel chromatography using $CHCl_3$/AcOEt (70:30 v/v) as eluent. The solid product **1j** was purified by crystallization (70% yield): mp 170−171 °C, from $CHCl_3$/*n*-hexane; ^{1}H NMR ($CDCl_3$) δ 7.25−7.32 (m, 4H), 7.37 (t, 2H, J = 7.7), 7.55 (tt, 1H, J = 7.5, 1.4), 7.62 (dd, 2H, J = 8.7, 1.4), 9.19 (d, 1H, J = 0.9), 9.36 (d, 1H, J = 0.9); IR (cm^{-1}) 1660, 835. Anal. ($C_{17}H_{11}ClN_2O$) C, H, N.

2-Methyl-9*H*-indeno[2,1-*d*]pyrimidine (2a′). 1-(*N*,*N*-Dimethylaminomethyliden)indan-2-one (0.187 g, 1.0 mmol)[27] was reacted with an excess of acetamidine hydrochloride (0.945 g, 10 mmol) and sodium methoxide (0.540 g, 10 mmol) in 10 mL of anhydrous EtOH under reflux for 48 h. The reaction mixture was filtered off and evaporated to dryness. The solid residue was dissolved in chloroform, and the organic solution was then washed with water, dried over Na_2SO_4, concentrated, and purified by chromatography on silica gel column using $CHCl_3$/AcOEt (60:40 v/v) as eluent, affording **2a′** as a yellow solid product in 47% yield: mp 121 °C (dec), from EtOH; ^{1}H NMR ($CDCl_3$) δ 2.79 (s, 3H), 3.95 (s, 2H), 7.33−7.44 (m, 2H), 7.54−7.59 (m, 1H), 7.76−7.79 (m, 1H), 8.93 (s, 1H); IR (cm^{-1}) 1585, 1405, 760. Anal. ($C_{12}H_{10}N_2$) C, H, N.

2-(3-Nitrophenyl)-9*H*-indeno[2,1-*d*]pyrimidine (2d′). Using 3-nitrobenzamidine hydrochloride (2.016 g, 10 mmol), through a procedure similar to that described for **2a′**, **2d′** was obtained after chromatographic separation (eluent: AcOEt/petroleum ether/*i*PrOH 50:50:1 v/v/v) as a yellow solid in 25% yield: mp 249 °C (dec), from EtOH/dioxane (80:20 v/v); ^{1}H NMR (DMSO-d_6) δ 4.26 (s, 2H), 7.51−7.56 (m, 2H), 7.72−7.77 (m, 1H), 7.89 (td, 1H, J = 8.2, 0.5), 8.12−8.17 (m, 1H), 8.42 (ddd, 1H, J = 8.2, 2.4, 1.1), 8.92 (ddd, 1H, J = 8.2, 1.6, 1.1), 9.24−9.26 (m, 1H), 9.50 (s, 1H); IR (cm^{-1}) 1526, 1347, 719. Anal. ($C_{17}H_{11}N_3O_2$) C, H, N.

2-Substituted-9*H*-indeno[2,1-*d*]pyrimidin-9-ones (2a,d). Compound **2a′** or **2d′** (0.25 mmol) was dissolved under magnetic stirring to reflux in 2.5 mL of acetic acid, and 48 mg of chromium(VI) oxide (0.48 mmol) was added. After 20 min, the solutions were allowed to cool to rt and poured onto crushed ice, and the yellow precipitates obtained (**2a** and **2d**) were filtered off, washed with water, and purified by crystallization.

2a (R′ = methyl): 50% yield; mp 150−151 °C from EtOH; ^{1}H NMR ($CDCl_3$) δ 2.83 (s, 3H), 7.38−7.44 (m, 1H), 7.54−7.59 (m, 2H), 7.77 (td, 1H, J = 7.1, 1.0), 8.91 (s, 1H); IR (cm^{-1}) 1730, 1410, 1105. Anal. ($C_{12}H_8N_2O$) C, H, N.

2d (R′ = 3-nitrophenyl): 74% yield; mp 208 °C (dec) from EtOH/dioxane (50:50 v/v); ^{1}H NMR ($CDCl_3$) δ 7.47 (td, 1H, J = 7.2, 1.7), 7.63−7.70 (m, 3H), 7.84 (dd, 1H, J = 7.3, 0.9), 8.35 (ddd, 1H, J = 8.2, 2.7, 1.0), 8.89 (td, 1H, J = 7.8, 1.4), 9.13 (s, 1H), 9.36 (t, 1H, J = 1.9); IR (cm^{-1}) 1734, 1529, 1349, 718. Anal. ($C_{17}H_9N_3O_3$) C, H, N.

5*H*-Indeno[1,2-*d*]pyrimidine (3c). 2-(*N*,*N*-Dimethylaminomethyliden)indan-1-one (0.187 g, 1.0 mmol)[27] was reacted with an excess of formamidine acetate (1.04 g, 10 mmol) as above-described for compounds **2a′**,**d′**. The crude reaction product was purified by silica gel chromatography using $CHCl_3$/MeOH/AcOEt (90:5:5 v/v/v) as eluent, affording a yellow solid product **3c** in 30% yield: mp 103−104 °C, from $CHCl_3$/*n*-hexane; ^{1}H NMR ($CDCl_3$) δ 3.94 (s, 2H), 7.50 (t, 1H, J = 7.5), 7.55 (td, 1H, J = 7.2, 1.5), 7.63 (d, 1H, J = 7.0), 8.15 (dd, 1H, J = 6.5, 1.7), 8.84 (s, 1H), 9.19 (s, 1H); IR (cm^{-1}) 1580, 1390, 735. Anal. ($C_{11}H_8N_2$) C, H, N.

4-Phenyl-5*H*-indeno[1,2-*d*]pyrimidin-5-one (3e). To a solution of 0.316 g of **3c** (2.0 mmol) in 12 mL of anhydrous THF under magnetic stirring in an ice bath was added dropwise a commercial solution of 1.6 M phenyllithium in cyclohexane/ether (2.5 mL) under N_2 atmosphere. After the addition, the mixture was kept at rt for 7 h, then poured onto 20 mL of saturated $NaHCO_3$ solution, and extracted several times with Et_2O. The collected Et_2O layers, washed with brine, were dried on Na_2SO_4 and evaporated to dryness. The solid residue was purified by silica gel chromatography using $CHCl_3$/MeOH/AcOEt (90:5:5 v/v/v) as eluent. Evaporation to dryness afforded 4-phenyl-5*H*-indeno[1,2-*d*]pyrimidine **3d** (28% yield), used for the subsequent reaction without further purification. Compound **3d** (0.060 g, 0.25 mmol) was oxidized with chromium(VI) oxide (0.48 mmol), and the product **3e** was purified by crystallization (56% yield): mp 155−156 °C from EtOH; ^{1}H NMR ($CDCl_3$) δ 7.49−7.62 (m, 4H), 7.69 (td, 1H, J = 7.4, 1.1), 7.78 (d, 1H, J = 7.3), 7.95 (d, 1H, J = 7.2), 8.14 (dd, 2H, J = 7.6, 1.9), 9.25 (s, 1H); IR (cm^{-1})1721, 1551, 758. Anal. ($C_{17}H_{10}N_2O$) C, H, N.

3-(3-Nitrophenyl)-9*H*-indeno[1,2-*e*][1,2,4]triazin-9-one (4c). Ninhydrin (0.534 g, 3 mmol) and 3-nitrobenzenecarboximidohydrazide (0.541 g, 3 mmol) were refluxed under magnetic stirring in 15 mL of anhydrous EtOH. After 30 min, the reaction mixture was cooled, and the precipitate obtained was filtered off and crystallized (89% yield): mp 244−245 °C, from EtOH/dioxane (85:15 v/v); ^{1}H NMR (DMSO-d_6) δ 7.85−7.98 (m, 4H), 8.26 (d, 1H, J = 7.4), 8.52 (dd, 1H, J = 8.1, 2.2), 8.97 (d, 1H, J = 8.1), 9.25 (t, 1H, J = 1.9); IR (cm^{-1}) 1729, 1568, 1346, 745. Anal. ($C_{16}H_8N_4O_3$) C, H, N.

3-(3-Aminophenyl)-9*H*-indeno[1,2-*e*][1,2,4]triazin-9-one (4b). Compound **4c** (0.304 g, 1.0 mmol) was reduced with tin(II) chloride (0.948 g, 5.0 mmol) in 100 mL of refluxing EtOH for 1.5 h. The reaction mixture was then evaporated to dryness and the residue extracted from water with $CHCl_3$. The organic layers, collected and washed with water, were dried over Na_2SO_4 and evaporated to dryness, to afford **4b** in 38% yield: mp 243−244 °C from EtOH; ^{1}H NMR (DMSO-d_6) δ 5.45 (d, 1H, J = 5.6), 6.84 (dd, 1H, J = 7.9, 1.8), 7.62 (t, 1H, J = 7.9), 7.73 (d, 1H, J = 7.9), 7.82−7.99 (m, 4H), 8.13 (dd, 1H, J = 7.2, 1.1), 8.30 (s, 1H); IR (cm^{-1}) 3464, 3358, 1758, 1490. Anal. ($C_{16}H_{10}N_4O$) C, H, N.

3-Phenyl-9*H*-indeno[1,2-*e*][1,2,4]triazin-9-one (4a). To a solution of *tert*-butyl nitrite (154 mg, 1.5 mmol) in 1 mL of anhydrous DMF kept to 70 °C was added slowly a solution of compound **4b** (0.160 g, 0.6 mmol) in 2 mL of anhydrous DMF over a period of 5 min with stirring. After 15 min, the deep red solution was allowed to cool to rt and poured into ice-cold 5% HCl. The yellow solid was filtered, washed with EtOH, and purified by crystallization (63% yield): mp >300 °C (dec at 159 °C) from EtOH; ^{1}H NMR

($CDCl_3$) δ 7.56−7.66 (m, 3H), 7.76 (td, 1H, J = 7.4, 1.1), 7.85 (td, 1H, J = 7.4, 1.1), 7.99 (d, 1H, J = 8.3), 8.19 (d, 1H, J = 7.4), 8.69−8.72 (m, 2H); IR (cm^{-1}) 1733, 1567, 1369, 753. Anal. ($C_{16}H_9N_3O$) C, H, N.

3-(3-Nitrophenyl)-5*H*-indeno[2,1-*e*][1,2,4]triazin-5-one (5). Indan-1,3-dione (0.146 g, 1 mmol) and 3-nitrobenzenecarboximidohydrazide (0.180 g, 1 mmol) were refluxed under magnetic stirring in 10 mL of anhydrous EtOH. After 2 h, the reaction mixture was cooled, and a solid product, having LC-MS and spectroscopic data consistent with those of the benzecarboximido hydrazide intermediate **5′**, was filtered off (79% yield). The crude product **5′** was used in the following reaction without further purification. Compound **5′** (92 mg, 0.3 mmol) was dissolved under magnetic stirring to reflux in 1 mL of glacial acetic acid, and then chromium (VI) oxide (42 mg, 0.42 mmol) was added. After 2 h, the solution was allowed to cool and poured onto 10 mL of ice-cold water. The brown precipitate was filtered and purified by silica gel chromatography using chloroform as eluent (71% yield): mp 225−7 °C (dec), from EtOH/dioxane (85:15 v/v); ^{1}H NMR (DMSO-d_6) δ 7.71 (td, 1H, J = 7.5, 1.2), 7.76 (t, 1H, J = 8.0), 7.87 (td, 1H, J = 7.5, 1.2), 7.99 (d, 1H, J = 7.5), 8.24 (d, 1H, J = 7.5), 8.44 (ddd, 1H, J = 8.4, 2.7, 1.2), 8.95 (dt, 1H, J = 7.8, 1.2), 9.45 (t, 1H, J = 2.7); IR (cm^{-1}) 1736, 1529, 1350, 718. Anal. ($C_{16}H_8N_4O_3$) C, H, N.

MAO Inhibition Assay. The newly synthesized compounds were tested for their inhibitory activity on MAO-A and -B in rat brain mitochondrial suspensions.[50] Incubations were carried out at pH 7.40 (Na_2HPO_4/KH_2PO_4 made isotonic with KCl) and 37 °C temperature. A continuous spectrophotometric assay that monitors the rate of oxidation of the nonselective MAO substrate kynuramine into 4-hydroxyquinoline was used.[51] Clorgyline (250 nm) or selegiline (250 nm) was preincubated with the suspension for 5 min to measure MAO-B or MAO-A activity, respectively. The formation of 4-hydroxyquinoline was followed at 314 nm using a Kontron UVIKON 941 spectrophotometer. The limited solubility of the tested compounds in aqueous solution required the use of 5% DMSO as cosolvent, a concentration that did not affect MAO activity. The substrate concentration used for the assays was 60 μM for MAO-B and 90 μM for MAO-A, corresponding to the respective K_M of kynuramine for the two isoenzymes. IC_{50} values were determined and calculated from a hyperbolic equation.[52] Each assay was performed in triplicate on four to six separate homogenates.

Acknowledgment. We thank Prof. Angelo Carotti (Bari, Italy) for insightful suggestions. A.C., M.C., F.L., F.C., and C.A. thank the Italian Ministry for Education Universities and Research (MIUR, Rome, Italy; PRIN 2004, Grant 2004037521_006) for financial support. R.S.-O. and E.M.-A. thank the Ministry of Education and Science, and the European Regional Development Fund (Madrid, Spain, Grant BFI2003-00493) for financial support.

Supporting Information Available: Table of elemental analyses (C, H, N) of the newly synthesized compounds and intermediates. This material is available free of charge via the Internet at http://pubs.acs.org.

References

(1) Tipton, K. F. Enzymology of monoamine oxidase. *Cell Biochem. Funct.* **1986**, *4*, 79−87.
(2) Nagatsu, T. Progress in monoamine oxidase (MAO) research in relation to genetic engineering. *Neurotoxicology* **2004**, *25*, 11−20.
(3) Shih, J. C. Cloning, after cloning, knock-out mice, and physiological functions of MAO-A and B. *Neurotoxicology* **2004**, *25*, 21−30.
(4) Testa, B.; Krämer, S. D. The biochemistry of drug metabolism − An introduction. Part 2: Redox reactions and their enzymes. *Chem. Biodiv.* **2007**, *4*, 257−405.
(5) Bach, A. W.; Lan, N. C.; Johnson, D. L.; Abell, C. W.; Bembenek, M. E.; Kwan, S. W.; Seeburg, P. H.; Shih, J. C. cDNA cloning of human liver monoamine oxidase A and B: Molecular basis of differences in enzymatic properties. *Proc. Natl. Acad. Sci. U.S.A.* **1988**, *85*, 4934−4938.
(6) Kwan, S. W.; Abell, C. W. cDNA cloning and sequencing of rat monoamine oxidase A: comparison with the human and bovine enzymes. *Comp. Biochem. Physiol. B* **1992**, *102*, 143−147.
(7) Kalgutkar, A. S.; Castagnoli, N., Jr.; Testa, B. Selective inhibitors of monoamine oxidase (MAO-A and MAO-B) as probes of its catalytic site and mechanism. *Med. Res. Rev.* **1995**, *15*, 325−388.
(8) Grimsby, J.; Lan, N. C.; Neve, R.; Chen, K.; Shih, J. C. Tissue distribution of human monoamine oxidase A and B mRNA. *J. Neurochem.* **1990**, *55*, 1166−1669.
(9) Riederer, P.; Lachenmayer, L.; Laux, G. Clinical applications of MAO-inhibitors. *Curr. Med. Chem.* **2004**, *11*, 2033−2043.
(10) Yamada, M.; Yasuhara, H. Clinical pharmacology of MAO inhibitors: safety and future. *Neurotoxicology* **2004**, *25*, 215−221.
(11) Palhagen, S.; Heinonen, E.; Hägglund, J.; Kaugesaar, T.; Mäki-Ikola, O.; Palm, R. Selegiline slows the progression of symptoms of Parkinson disease. *Neurology* **2006**, *66*, 1200−1206.
(12) Riederer, P.; Danielczyk, W.; Grunblatt, E. Monoamine oxidase-B inhibition in Alzheimer's disease. *Neurotoxicology* **2004**, *25*, 271−277.
(13) Youdim, M. B. H.; Fridkin, M.; Zheng, H. Novel bifunctional drugs targeting monoamine oxidase inhibition and iron chelation as an approach to neuroprotection in Parkinson's disease and other neurodegenerative diseases. *J. Neural Transm.* **2004**, *3*, 205−214.
(14) Wouters, J. Structural aspects of monoamine oxidase and its reversible inhibition. *Curr. Med. Chem.* **1998**, *5*, 137−162.
(15) Shih, J. C.; Chen, K.; Geha, R. M. Determination of regions important for monoamine oxidase (MAO) A and B substrate and inhibitor selectivities. *J. Neural. Transm. Suppl.* **1998**, *52*, 1−8.
(16) Gottowik, J.; Malherbe, P.; Lang, G.; Da Prada, M.; Cesura, A. M. Structure/function relationships of mitochondrial monoamine oxidase A and B chimeric forms. *Eur. J. Biochem.* **1995**, *230*, 934−942.
(17) De Colibus, L.; Li, M.; Binda, C.; Lustig, A.; Edmondson, D. E.; Mattevi, A. Three-dimensional structure of human monoamine oxidase A (MAO-A): Relation to the structures of rat MAO-A and human MAO-B. *Proc. Natl. Acad. Sci. U.S.A.* **2005**, *102*, 12684−12689.
(18) Binda, C.; Newton-Vinson, P.; Hubalek, F.; Edmondson, D. E.; Mattevi, A. Structure of human monoamine oxidase B, a drug target for the treatment of neurological disorders. *Nat. Struct. Biol.* **2002**, *9*, 22−26.
(19) Binda, C.; Hubalek, F.; Li, M.; Herzig, Y.; Sterling, J.; Edmondson, D. E.; Mattevi, A. Crystal structures of monoamine oxidase B in complex with four inhibitors of the *N*-propargylaminoindane class. *J. Med. Chem.* **2004**, *47*, 1767−1774.
(20) Binda, C.; Li, M.; Hubalek, F.; Restelli, N.; Edmondson, D. E.; Mattevi, A. Insights into the mode of inhibition of human mitochondrial monoamine oxidase B from high-resolution crystal structures. *Proc. Natl. Acad. Sci. U.S.A.* **2003**, *100*, 9750−9755.
(21) Edmondson, D. E.; Mattevi, A.; Binda, C.; Li, M.; Hubalek, F. Structure and mechanism of monoamine oxidase. *Curr. Med. Chem.* **2004**, *11*, 1983−1993.
(22) Carrieri, A.; Carotti, A.; Barreca, M. L.; Altomare, C. Binding models of reversible inhibitors to type-B monoamine oxidase. *J. Comput.-Aided Mol. Des.* **2002**, *16*, 769−778.
(23) Novaroli, L.; Daina, A.; Favre, E.; Bravo, J.; Carotti, A.; Leonetti, F.; Catto, M.; Carrupt, P.-A.; Reist, M. Impact of species-dependent differences on screening, design, and development of MAO-B inhibitors. *J. Med. Chem.* **2006**, *49*, 6264−6272.
(24) Kneubühler, S.; Carta, V.; Altomare, C.; Carotti, A.; Testa, B. Synthesis and monoamine oxidase inhibitory activity of 3-substituted 5*H*-indeno[1,2-*c*]pyridazines. *Helv. Chim. Acta* **1993**, *76*, 1954−1963.
(25) Kneubühler, S.; Thull, U.; Altomare, C.; Carta, V.; Gaillard, P.; Carrupt, P.-A.; Carotti, A.; Testa, B. Inhibition of monoamine oxidase-B by 5*H*-indeno[1,2-*c*]pyridazines: biological activities, quantitative structure−activity relationships (QSARs) and 3D-QSARs. *J. Med. Chem.* **1995**, *38*, 3874−3883.
(26) Thull, U.; Kneubühler, S.; Gaillard, P.; Carrupt, P.-A.; Testa, B.; Altomare, C.; Carotti, A.; Jenner, P.; McNaught, K. St. P. Inhibition of monamine oxidase by isoquinoline derivatives: qualitative and 3D-quantitative structure-activity relationships. *Biochem. Pharmacol.* **1995**, *50*, 869−877.
(27) Altomare, C.; Cellamare, S.; Summo, L.; Catto, M.; Carotti, A.; Thull, U.; Carrupt, P.-A.; Testa, B.; Stoekli-Evans, H. Inhibition of monoamine oxidase-B by condensed pyridazines and pyrimidines; effects of lipophilicity and structure−activity relationships. *J. Med. Chem.* **1998**, *41*, 3812−3820.
(28) Gnerre, C.; Catto, M.; Leonetti, F.; Weber, P.; Carrupt, P.-A.; Altomare, C.; Carotti, A.; Testa, B. Inhibition of monoamine oxidases by functionalized coumarin derivatives: biological activities, QSARs, and 3D-QSARs. *J. Med. Chem.* **2000**, *43*, 4747−4758.

(29) Carotti, A.; Carrieri, A.; Chimichi, S.; Boccalini, M.; Cosimelli, S.; Gnerre, C.; Carotti, A.; Carrupt, P.-A., Testa, B. Natural and synthetic geiparvarins are strong and selective MAO-B inhibitors. Synthesis and SAR studies. *Bioorg. Med. Chem. Lett.* **2002**, *12*, 3551−3555.
(30) Novaroli, L.; Reist, M.; Favre, E.; Carotti, A.; Catto, M.; Carrupt, P.-A. Human recombinant monoamine oxidase B as reliable and efficient enzyme source for inhibitor screening. *Bioorg. Med. Chem.* **2005**, *13*, 6212−6217.
(31) Carotti, A.; Altomare, C.; Catto, M.; Gnerre, C.; Summo, L.; De Marco, A.; Rose, S.; Jenner, P.; Testa, B. Lipophilicity plays a major role in modulating the inhibition of monoamine oxidase B by 7-substituted coumarins. *Chem. Biodiv.* **2006**, *3*, 134−149.
(32) Catto, M.; Nicolotti, O.; Leonetti, F.; Favia, A. D.; Soto-Otero, R.; Méndez-Alvarez, E.; Carotti, A. Structural insights into monoamine oxidase inhibitory potency and selectivity of 7-substituted coumarins from ligand- and target-based approaches. *J. Med. Chem.* **2006**, *49*, 4912−4925.
(33) Ooms, F.; Frédérick, R.; Durant, F.; Petzer, J. P.; Castagnoli, N., Jr.; Van der Schyf, J.; Wouters, J. Rational approaches towards reversible inhibition of type B monoamine oxidase. Design and evaluation of a novel 5*H*-indeno[1,2-*c*]pyridazin-5-one derivative. *Bioorg. Med. Chem. Lett.* **2003**, *12*, 69−73.
(34) Frédérick, R.; Dumont, W.; Ooms, F.; Aschenbach, L.; Van der Schyf, J.; Castagnoli, N.; Wouters, J.; Krief, A. Synthesis, structural reassignment, and biological activity of type B inhibitors based on the 5*H*-indeno[1,2-*c*]pyridazin-5-one core. *J. Med. Chem.* **2006**, *49*, 3743−3747.
(35) Cignarella, G.; Loriga, M.; Pinna, G. A.; Pirisi, M. A.; Schiatti, P.; Selva, D. Unexpected anti-inflammatory activity of rigid structures derived from antihypertensive 6-arylpyridazinones. III. Synthesis and activity of 7-fluoro- and 5-keto-5*H*-indeno[1,2-*c*]pyridazines. *Farmaco* **1982**, *37*, 133−144.
(36) Heinish, G.; Jentzsch, A.; Pailer, M. C-4 substituted pyridazines by homolitic alkylation and acylation. *Monatsh. Chem.* **1974**, *105*, 648−652.
(37) Case, F. H. The action of diphenyl triketone and of ninhydrin on certain carboxamide hydrazones. *J. Heterocycl. Chem.* **1972**, *9*, 457−458.
(38) Campagna, F.; Palluotto, F.; Mascia, M. P.; Ma ciocco, E.; Marra, C.; Carotti, A.; Carrieri, A. Synthesis and biological evaluation of pyridazino[4,3-*b*]indoles and indeno[1,2-*c*]pyridazines as new ligands of central and peripheral benzodiazepine receptors. *Farmaco* **2003**, *58*, 129−140.
(39) Ghigi, E. Su alcuni omologhi nucleari del carbazolo idrogenato e derivati pirazolonici dell'a-tetralone (On some nuclear homologues of hydrogenated carbazole and pyrazolone derivatives of a-tetralone). *Gazz. Chim. Ital.* **1930**, *60*, 194−199.
(40) Pappa, H.; Segall, A.; Pizzorno, M. T.; Radice, M.; Amoroso, A.; Gutkind, G. O. Antimicrobial activity of 5,6-dihydrobenzo[*a*]carbazoles. *Farmaco* **1994**, *49*, 333−336.
(41) Medvedev, A. E.; Veselovsky, A. V.; Shvedov, V. I.; Tikhonova, O. V.; Moskvitina, T. A.; Fedotova, O. A.; Axenova, L. N.; Kamyshanskaya, N. S.; Kirkel, A. Z.; Ivanov, A. S. Inhibition of monoamine oxidase by pirlindole analogues: 3D-QSAR and CoMFA analysis. *J. Chem. Inf. Comput. Sci.* **1998**, *38*, 1137−1144.
(42) Altomare, C.; Carrupt, P.-A.; Gaillard, P.; El Tayar, N.; Testa, B.; Carotti, A. Quantitative structure-metabolism relationship analyses of MAO-mediated toxication of 1-methyl-4-phenyl-1,2,3,6-tetrahydropyridine and analogues. *Chem. Res. Toxicol.* **1992**, *5*, 366−375.
(43) Lipophilicity was assessed by calculating 1-octanol/water log *P* values with ACDLabs software, release 7.0 (Advanced Chemistry Development Inc., Toronto, Canada). Compound **1k** has calculated log *P* of 1.44, whereas the indeno-azine derivatives showing the highest MAO-B inhibition potency in the series (IC_{50} < 10 μM) have log *P* values ranging from 2.44 (**2a**) to 3.57 (**4a**).
(44) McMartin, C.; Bohacek, R.S. QXP: powerful, rapid computer algorithms for structure-based drug design. *J. Comput. Aid.-Mol. Des.* **1997**, *11*, 333−344. The molecular model of **4c** was built with the QXP editor and minimized using the default protocol (300 iterations, energy cut-off of 0.1 kJ·mol^{-1}, Polak-Ribiere conjugate gradient). The ligand-free protein and cofactor were kept rigid, except for the side chains of the residues lying within a distance of 4 Å from 1,4-diphenyl-2-butene in the original pdb complex (1oj9) retrieved by the Brookhaven Protein Data Bank (http://www.rcsb.org/pdb/), which were settled free to relax during the minimization of the binding complexes found by the calculation routine. Finally, phenol oxygen atom of Y398 was marked for indicating the binding cavity, and the inhibitor added and settled as completely free to move. To allow a good sampling of the conformational space, 1000 runs of Monte Carlo search, followed by conjugate gradient minimization, were performed, and the first-scored 25 low-energy docking hypotheses were taken into account.
(45) Warren, L. The PyMOL Molecular Graphics System, DeLano Scientific LLC, San Carlos, CA; http://www.pymol.org.
(46) Verdonk, M. L.; Cole, J. C.; Hartshorn, M. J.; Murray, C. W.; Taylor, R. D. Improved protein−ligand docking using GOLD. *Proteins: Struct., Funct., Genet.* **2003**, *52*, 609−623.
(47) Gaillard, P.; Carrupt, P.-A.; Testa, B.; Boudon, A. Molecular lipophilicity potential, a tool in 3D-QSAR. Method and applications. *J. Comput.-Aided Mol. Des.* **1994**, *8*, 83−96.
(48) Hynson, R. M. G.; Wouters, J.; Ramsay, R. R. Monoamine oxidase A inhibitory potency and flavin perturbation are influenced by different aspects of pirlindole inhibitor structure. *Biochem. Pharmacol.* **2003**, *65*, 1867−1874.
(49) Imamoto, T.; Takiyama, N.; Nakamura, K. Cerium chloride-promoted nucleophilic addition of Grignard reagents to ketones. An efficient method for the synthesis of tertiary alcohols. *Tetrahedron Lett.* **1985**, *26*, 4763−4766.
(50) Clark, J. B.; Nicklas, W. J. The metabolism of rat brain mitochondria. *J. Biol. Chem.* **1970**, *245*, 4724−4731.
(51) Weissbach, H.; Smith, T. E.; Daly, J. W.; Witkop, B.; Udenfriend, S. A rapid spectrophotometric assay of monoamine oxidase based on the rate of disappearance of kynuramine. *J. Biol. Chem.* **1960**, *235*, 1160−1163.
(52) Thull, U.; Kneubühler, S.; Testa, B.; Borges, M. F. M.; Pinto, M. M. M. Substituted xanthones as selective and reversible monoamine oxidase A (MAO-A) inhibitors. *Pharm. Res.* **1993**, *10*, 1187−1190.

JM070728R